

## A 700 W·h·kg<sup>-1</sup> Rechargeable Pouch Type Lithium Battery

Quan Li(李泉)<sup>1,2</sup>, Yang Yang(杨旸)<sup>1,2,3</sup>, Xiqian Yu(禹习谦)<sup>1,2,3\*</sup>, and Hong Li(李泓)<sup>1,2,3\*</sup>

<sup>1</sup>Beijing National Laboratory for Condensed Matter Physics, and Institute of Physics,  
Chinese Academy of Sciences, Beijing 100190, China

<sup>2</sup>Huairou Division, Institute of Physics, Chinese Academy of Sciences, Beijing 101400, China

<sup>3</sup>Center of Materials Science and Optoelectronics Engineering, University of Chinese Academy of Sciences,  
Beijing 100049, China

(Received 3 March 2023; accepted manuscript online 17 March 2023)

High-energy-density rechargeable lithium batteries are being pursued by researchers because of their revolutionary potential nature. Current advanced practical lithium-ion batteries have an energy density of around 300 W·h·kg<sup>-1</sup>. Continuing to increase the energy density of batteries to a higher level could lead to a major explosion development in some fields, such as electric aviation. Here, we have manufactured practical pouch-type rechargeable lithium batteries with both a gravimetric energy density of 711.3 W·h·kg<sup>-1</sup> and a volumetric energy density of 1653.65 W·h·L<sup>-1</sup>. This is achieved through the use of high-performance battery materials including high-capacity lithium-rich manganese-based cathode and thin lithium metal anode with high specific energy, combined with extremely advanced process technologies such as high-loading electrode preparation and lean electrolyte injection. In this battery material system, the structural stability of cathode material in a widened charge/discharge voltage range and the deposition/dissolution behavior of interfacial modified thin lithium electrode are studied.

DOI: 10.1088/0256-307X/40/4/048201

Advanced lithium battery is the key technology for achieving the high-efficiency utilization of clean energy and the increasing electrification of transportation sectors, promoting the realization of carbon peaking and carbon neutrality goals.<sup>[1,2]</sup> Accordingly, major countries have put forward blueprints to develop advanced lithium batteries, e.g., the National Blueprint for Lithium Batteries 2021–2030 and the Battery Innovation Roadmap 2030 proposed by the United States and Europe, in which the battery energy density has been used as a primary reference for policy formulation, with an energy density of 500 W·h·kg<sup>-1</sup> as a long-term objective.<sup>[3,4]</sup> Importantly, further increasing the energy density of lithium batteries will expand its applications to the field of electric aviation, which has been attracting broad attention. Recently, a key consulting project has been launched by the Chinese Academy of Engineering, and a white paper has been released by the Department of Energy of the United States, focusing on the R&D needs for electric aviation from the aspect of energy storage systems.<sup>[5,6]</sup>

Since the lithium-ion battery has been first commercialized by Sony in 1991, its energy density has increased from 80 W·h·kg<sup>-1</sup> to 300 W·h·kg<sup>-1</sup> at the cell level,<sup>[7]</sup> enabling lithium-ion batteries to be widely used in 3C (computer, communication, and consumer electronics) and electric vehicles. At present, the most reliable commercial batteries employ intercalation-type cathodes (e.g., LiFePO<sub>4</sub>, LiCoO<sub>2</sub>, LiNi<sub>x</sub>Mn<sub>y</sub>Co<sub>z</sub>O<sub>2</sub>,  $x + y + z = 1$ ) and graphite-based anodes, whose energy density, however, has been approaching its upper limit. Continuous efforts have been made to develop rechargeable lithium batteries with

higher energy density by using novel high-capacity electrode materials and advanced battery technologies. For example, Louli *et al.* reported an anode-free battery using the layered oxide LiNi<sub>0.8</sub>Mn<sub>0.1</sub>Co<sub>0.1</sub>O<sub>2</sub> (NMC811) as a cathode. The cell achieved a gravimetric energy density of 575 W·h·kg<sup>-1</sup> and a volumetric energy density of 1414 W·h·L<sup>-1</sup>, reaching the highest level reported to date.<sup>[8]</sup> Nevertheless, the cyclic performances as well as other performance indexes (e.g., power and safety) degrade significantly with the increase in energy density.

There are many obstacles to further improving the energy density of practical batteries. On the one hand, enhancing the specific energy of active substances is the primary challenge. For the layered oxide cathodes, the specific energy can be enhanced by increasing the extractable lithium content or widening the working voltage range;<sup>[9]</sup> while for the anodes, increasing the specific capacity of lithium storage and reducing the electrode potential are effective methods.<sup>[10]</sup> However, when the cathode and anode are in a high lithiation or de-lithiation state, poor stability is a critical issue, manifested by the cathode structure collapse,<sup>[11]</sup> side reactions at the interface,<sup>[12]</sup> huge volume changes of the anode,<sup>[13]</sup> leading to the failure of the electrode active substances. Meanwhile, the electrolyte may suffer from redox decomposition when widening the working voltage range of the electrodes,<sup>[14]</sup> affecting the electrochemical performance of the practical batteries. Overall, crucial battery materials like the cathode, anode, and electrolyte, as well as their stabilities, are the key factors determining the feasibility and practicability of high-energy-density lithium batteries.

\*Corresponding author. Email: xyu@iphy.ac.cn; hli@iphy.ac.cn  
© 2023 Chinese Physical Society and IOP Publishing Ltd

On the other hand, reducing the proportion of auxiliary materials is another vital challenge to increasing the energy density of practical batteries. Commonly available strategies<sup>[15–18]</sup> include increasing the thickness of active electrode substances, reducing the amount of electrolyte usage, optimizing the proportion of electrode paste, reducing the areal density of the separator, and adopting lightweight current collectors. Unfortunately, most of those methods face practical challenges. For instance, in a thick electrode the Li-ion transport will be affected due to the high tortuosity and long diffusion path,<sup>[19]</sup> and it is also technically difficult to achieve high coating uniformity and high adhesion to current collectors. Reducing the amount of the electrolytes may lead to an early depletion of electrolytes or even an insufficient wetting between electrolytes and electrodes, deteriorating Li-ion transport.<sup>[20,21]</sup> Therefore, to realize the preparation of ultra-high energy density practical lithium batteries, it is necessary to comprehensively consider both the critical materials and the engineering technology.

In this work, we have manufactured practical pouch-type rechargeable lithium batteries using high-capacity  $\text{Li}_{1.2}\text{Ni}_{0.13}\text{Co}_{0.13}\text{Mn}_{0.54}\text{O}_2$  cathode and lithium metal an-

ode. The as-made batteries exhibit a gravimetric energy density of  $711.3 \text{ W}\cdot\text{h}\cdot\text{kg}^{-1}$  and a volumetric energy density of  $1653.65 \text{ W}\cdot\text{h}\cdot\text{L}^{-1}$ , which are the highest in rechargeable lithium batteries based on the intercalation-type cathode. We explore the energy density improvement and structural stability of lithium-rich cathode under a variety of charge/discharge voltage ranges. Further, we also investigate the balance between energy density and cycling performance of lithium anodes with different thicknesses and optimize the cycling performance of large surface capacity lithium anodes through interface modifications. The technical combination of high mass loading cathode, thin lithium anode, current collectors of  $6 \mu\text{m}$  Cu foil and  $9 \mu\text{m}$  Al foil, and lean electrolyte makes the mass ratio of cathode active substances reach more than 60%, much higher than that in commercialized lithium-ion batteries ( $\sim 48\%$ ). Overall, through the comprehensive optimization and combination of materials system and manufacturing technology, we achieve the preparation of ultra-high energy density practical lithium batteries, and our work will further lead research, development, and applications of ultra-high energy density lithium batteries in various fields.

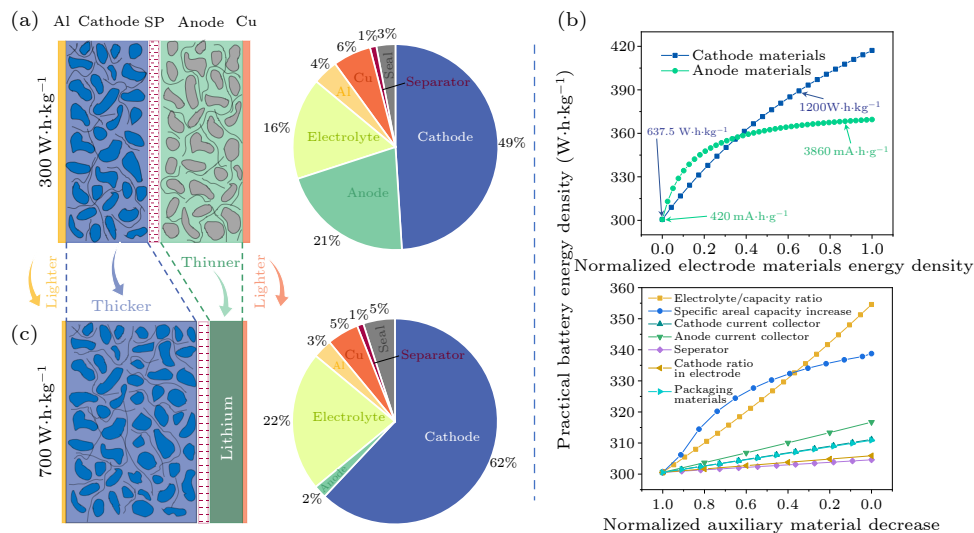


**Fig. 1.** Batteries design: (a) the mass constitution of the existing  $300 \text{ W}\cdot\text{h}\cdot\text{kg}^{-1}$  commercial lithium-ion battery, (b) the increase of energy density in practical lithium batteries by increasing active electrode materials' energy density and decreasing auxiliary materials' mass, (c) the mass construction of a  $700 \text{ W}\cdot\text{h}\cdot\text{kg}^{-1}$  battery involved in this work.

At present, the energy density of advanced commercial lithium-ion batteries has reached the level of  $300 \text{ W}\cdot\text{h}\cdot\text{kg}^{-1}$ . Those batteries are mainly composed of cathodes such as  $\text{LiCoO}_2$  (LCO), lithium Nickel Manganese Cobalt (NMC) oxide series, and matched anodes like graphite, hard carbon, and low-content silicon-base materials. Due to a comprehensive consideration of cycling performance, rate performance, safety, environmental adaptability, etc., the proportion of active cathode materials is always low, at the level of 50%, while the proportion of anode materials accounts for 18%–25% and other auxiliary materials take up 25%–30% of the total mass [Fig. 1(a)]. Disregarding all the other aspects, only focusing on energy density, approaches like adopting cath-

ode and anode materials with higher specific energy, increasing electrode loading mass, reducing the ratio of electrolyte mass and battery capacity ( $E/C$ ), and adopting lighter and thinner collectors, separators, packaging materials, etc. are all feasible to achieve a high value of energy density. After analyzing the design of the existing  $300 \text{ W}\cdot\text{h}\cdot\text{kg}^{-1}$  battery thoroughly, we calculate the dependence between energy density and several main components regardless of the normal functionality of the batteries. The results show that cathode and anode materials, loading mass, and  $E/C$  ratio are dominant in improving energy density. On the one hand, the battery energy density increases linearly with the decrease of the electrolyte mass, the current collectors' thickness, the separator areal

density, and the weight of the sealing material. On the other hand, the battery energy density increases linearly with the specific capacity of the cathode/anode and the area loading mass of the electrode, before tending to a constant. Unfortunately, the change of every single component cannot warrant the battery to reach an energy density of above  $400 \text{ W}\cdot\text{h}\cdot\text{kg}^{-1}$  [Fig. 1(b)]. The fabrication of high-energy density batteries can only be achieved by the synergy of up-mentioned factors (Fig. S1 in the Supplemen-

tal Materials). For instance, a practical design enabling battery energy density to exceed  $500 \text{ W}\cdot\text{h}\cdot\text{kg}^{-1}$  is replacing the cathode and anode with lithium-rich manganese-based (LRM) and Li metal. Furthermore, by increasing LRM loading mass to  $10 \text{ mA}\cdot\text{h}\cdot\text{cm}^{-2}$  (calculated by  $300 \text{ mA}\cdot\text{h}\cdot\text{g}^{-1}$ ) and decreasing the E/C ratio to less than  $1.5 \text{ g}\cdot\text{A}^{-1}\cdot\text{h}^{-1}$ , leading to the mass proportion of LRM surpassing 60%, eventually, the battery energy density could reach an unprecedented  $620\text{--}700 \text{ W}\cdot\text{h}\cdot\text{kg}^{-1}$  [Fig. 1(c)].

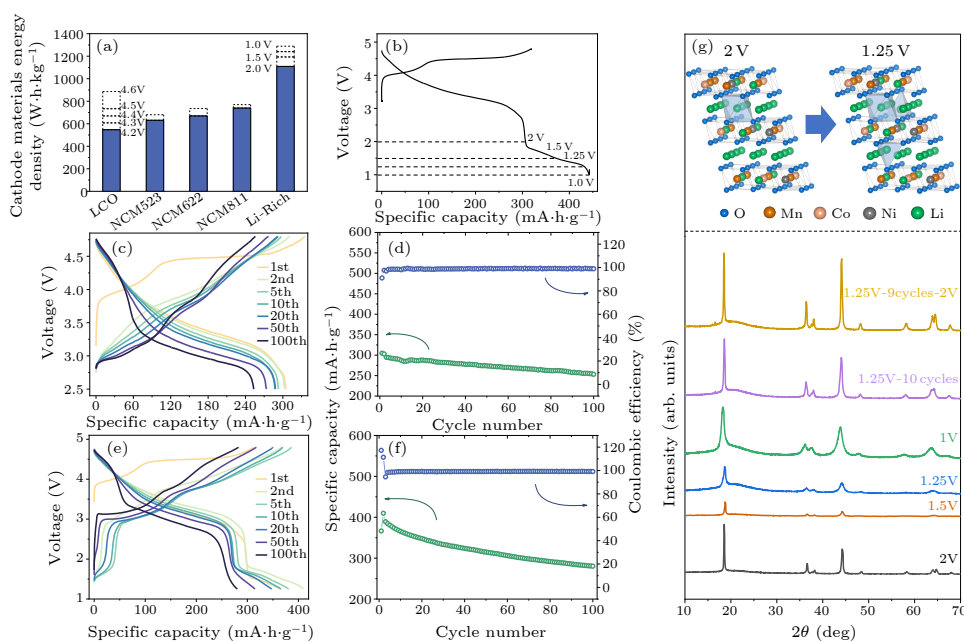


**Fig. 2.** LRM under the widened cut-off voltage range: (a) the energy density release of various transition metal oxide cathode materials at different charging cut-off voltages, (b) the first charge-discharge curve of  $\text{Li}_{1.2}\text{Ni}_{0.13}\text{Co}_{0.13}\text{Mn}_{0.54}\text{O}_2$  in the 1.0–4.8 V voltage range, (c) charge/discharge curves of the 1<sup>st</sup>, 2<sup>nd</sup>, 5<sup>th</sup>, 10<sup>th</sup>, 20<sup>th</sup>, 50<sup>th</sup>, and 100<sup>th</sup> cycles at 2.5–4.8 V, (d) cycling performance at 2.5–4.8 V, (e) charge/discharge curves of the 1<sup>st</sup>, 2<sup>nd</sup>, 5<sup>th</sup>, 10<sup>th</sup>, 20<sup>th</sup>, 50<sup>th</sup>, 100<sup>th</sup> cycles at 1.25–4.8 V, (f) cycling performance at 1.25–4.8 V, (g) the structure stability of  $\text{Li}_{1.2}\text{Ni}_{0.13}\text{Co}_{0.13}\text{Mn}_{0.54}\text{O}_2$  at different discharging cut-off voltages and at the 10<sup>th</sup> cycle.

The specific energy of the cathode material is the most important factor to determine the energy density of the battery as the mass proportion of the cathode is the highest in a battery. Among the current commercialized cathode materials, the specific energy of transition metal oxide cathode increases with the extractable lithium content. For LCO and NMC series cathode materials, although expanded cut-off voltage could increase the specific energy, the improvement of energy density is still limited, unable to exceed  $900 \text{ W}\cdot\text{h}\cdot\text{kg}^{-1}$  at the level of the material [Fig. 2(a)]. In comparison, the LRM cathode holds the highest energy density of more than  $1100 \text{ W}\cdot\text{h}\cdot\text{kg}^{-1}$  in the normal range of working voltage. Meanwhile, based on recent research, the LRM materials exhibit structural reversibility in a widened charge-discharge voltage range.<sup>[22,23]</sup> With a reversible characteristic of LRM, the increase of specific energy with an expanded voltage range is valuable to explore. When the cut-off voltage drops from 2 V to 1 V, the discharge specific capacity of LRM delivers from  $300 \text{ mA}\cdot\text{h}\cdot\text{g}^{-1}$  to  $442.8 \text{ mA}\cdot\text{h}\cdot\text{g}^{-1}$ , and the highest specific energy can reach  $1288.9 \text{ W}\cdot\text{h}\cdot\text{kg}^{-1}$  in a half cell in the 1–4.8 V range [Fig. 2(b)]. In terms of cycling performance, the coin cells with Li metal as an anode can remain

a capacity of more than  $250 \text{ mA}\cdot\text{h}\cdot\text{g}^{-1}$  after 100 cycles in the voltage range of 2.5–4.8 V [Fig. 2(c)], while this value exceeds  $280 \text{ mA}\cdot\text{h}\cdot\text{g}^{-1}$  when the discharge cut-off voltage is 1.25 V [Fig. 2(e)], corresponding to a capacity retention of 86.12% and 72.05%, respectively. In addition, the high coulombic efficiency of more than 99% is maintained during the long cycle process by reducing the discharge cut-off voltage [Figs. 2(d) and 2(f)]. The widened voltage range would accelerate the decay of the cathode specific capacity, which may be caused by the distorted structure during excessive  $\text{Li}^+$  intercalation/deintercalation. To validate the relationship between the performance decay and the structure evolution, further study on LRM cathode by XRD at different cut-off voltages was performed [Fig. 2(g)]. From the results, when the lithium ion is intercalated below 1.5 V, the layered structure remains stable though some lithium ions enter the tetrahedral positions. After the battery is charged and discharged within the voltage range of 1.25–4.8 V for 10 cycles, the layered structure of the material could still be maintained when the voltage stopped at 1.25 V (purple line) and 2 V (yellow line). The appreciable structural reversibility could be further confirmed by tracking the variation of lattice parameters, as shown in

Fig. S2. Only 0.002% and 0.016% changes of lattice parameters  $a$  and  $c$  could be observed after 10 electrochemical cycles.

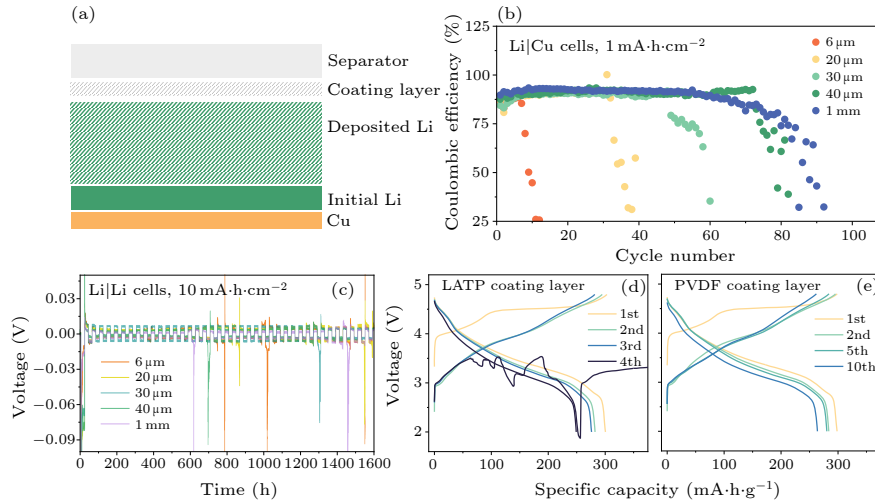


**Fig. 3.** Thickness dependence and interfacial modification of lithium metal anode: (a) the illustration of lithium metal anode interfacial modification, (b) cycling performance of metallic lithium of various thicknesses in Li|Cu cells, (c) polarization curves of metallic lithium of various thicknesses in Li|Li cells with  $10 \text{ mA}\cdot\text{h}\cdot\text{cm}^{-2}$ , (d) charge/discharge curves of  $\text{Li}_{1.2}\text{Ni}_{0.13}\text{Co}_{0.13}\text{Mn}_{0.54}\text{O}_2|\text{Li}$  cell with LAMP coating layer adjoined Li, (e) charge/discharge curves of  $\text{Li}_{1.2}\text{Ni}_{0.13}\text{Co}_{0.13}\text{Mn}_{0.54}\text{O}_2|\text{Li}$  cell with the PVDF coating layer adjoined Li.

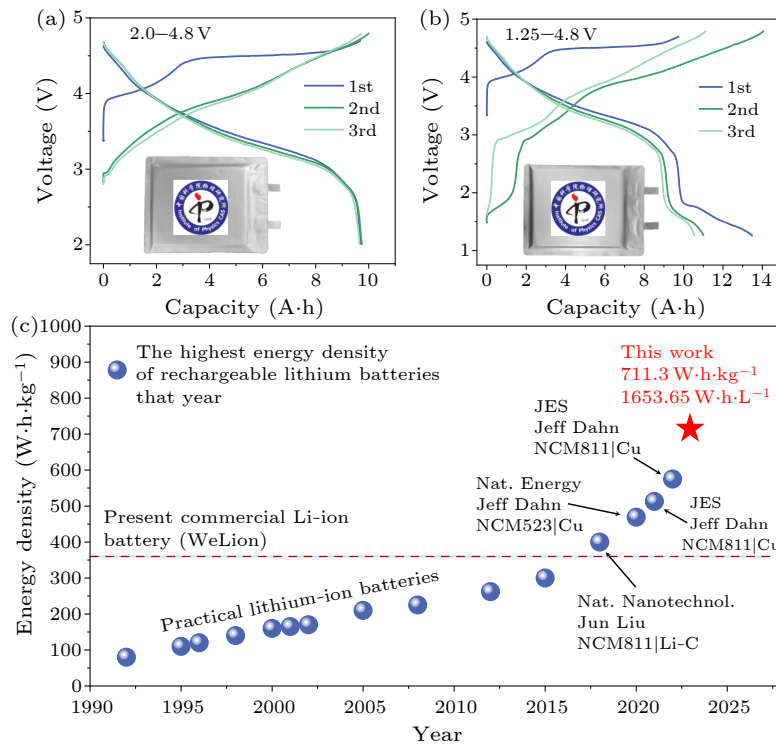


**Fig. 4.** Charge-discharge curves of the  $700 \text{ W}\cdot\text{h}\cdot\text{kg}^{-1}$   $\text{Li}_{1.2}\text{Ni}_{0.13}\text{Co}_{0.13}\text{Mn}_{0.54}\text{O}_2|\text{Li}$  pouch cell ( $\sim 10 \text{ A}\cdot\text{h}$ ) at (a) 2.0–4.8 V and (b) 1.25–4.8 V. (c) Comparison of the energy density of rechargeable intercalation-type cathode pouch cells in recent 30 years. [8,17,24–26]

Another well-acknowledged method to reach a high level of energy density is to apply lithium metal as an anode. However, lithium metal anodes face many problems in practical applications during lithium deposition [Fig. 3(a)], including lithium dendrites, volume expansion, high chemical reactivity, etc., especially under a large-

area capacity condition. [27] Those issues will degrade the cycling performance and safety of the battery, especially when the thickness of the lithium metal decreases. [28] Obviously, the thickened lithium would significantly downgrade the energy density of the battery, so that there is an optimal lithium thickness for co-optimization of en-

ergy density and cycling performance. Based on the aforementioned  $700 \text{ W}\cdot\text{h}\cdot\text{kg}^{-1}$  battery design, the thickness of lithium metal needs to be less than  $50 \mu\text{m}$ . Hence, lithium plates with different thicknesses from  $6 \mu\text{m}$  to  $1 \text{ mm}$  were employed to study the deposition and dissolution behavior. As shown in Fig. 3(b), for Li|Cu cells with  $1 \text{ mA}\cdot\text{h}\cdot\text{cm}^{-2}$  specific area capacity, it can be found that the coulombic efficiency of a  $6 \mu\text{m}$  lithium foil decay significantly after only 8 cycles, while all the other samples cycle more than 30 times. Hence, the application of  $20 \mu\text{m}$  lithium metal in the battery can achieve high energy density while maintaining suitable recyclability at the same time. To evaluate the cycling performance with a specific area capacity of  $10 \text{ mA}\cdot\text{h}\cdot\text{cm}^{-2}$  ( $48.5 \mu\text{m}$  lithium), we choose the Li|Li cells as the system instead of Li|Cu cells. As anticipated, the cycling performance becomes worse at large-area specific capacity. To our surprise, unlike the Li|Cu cells, the thinner lithium, the later voltage jitter occurs in the Li|Li cells. To further improve the reversibility of lithium deposition and dissolution, we coated organic (polyvinylidene difluoride, PVDF) and inorganic ( $\text{Li}_{1.3}\text{Al}_{0.3}\text{Ti}_{1.7}(\text{PO}_4)_3$ , LATP) interface layers on the separator respectively to explore the effect of the interface [Fig. 3(a)]. It is found that the organic interface layer of PVDF is more stable to guide lithium deposition/dissolution much more uniformly [Fig. 3(d)], whereas the inorganic interface layer of LATP cannot be charged/discharged normally after the fourth cycle [Fig. 3(e)].

Based on the high specific capacity LRM cathode with widened voltage range and  $20 \mu\text{m}$  Li metal anode stabilized by PVDF separator, we fabricate practical soft pack lithium batteries. Matching with the extreme manufacturing techniques, the one-sided specific area capacity of the cathode exceeds  $10 \text{ mA}\cdot\text{h}\cdot\text{cm}^{-2}$ , and the compact density is greater than  $2.6 \text{ g}\cdot\text{cm}^{-3}$ . Moreover, the current collectors are made of ultra-thin Al ( $9 \mu\text{m}$ ) & Cu ( $6 \mu\text{m}$ ) foil, and the  $E/C$  ratio is  $1.3 \text{ g}\cdot\text{A}^{-1}\cdot\text{h}^{-1}$ . Within the routine charge-discharge voltage range of  $2\text{--}4.8 \text{ V}$ , the  $9.72 \text{ A}\cdot\text{h}$  full battery exhibits  $601.78 \text{ W}\cdot\text{h}\cdot\text{kg}^{-1}$  gravimetric energy density and more than  $1175.56 \text{ W}\cdot\text{h}\cdot\text{L}^{-1}$  volumetric energy density [Fig. 4(a)], and the battery discharge capacity has no obvious decline after 3 cycles. Further extending the operating voltage range to  $1.25\text{--}4.8 \text{ V}$ , the energy contained in the low voltage interval assists the gravimetric energy density up to  $701.06 \text{ W}\cdot\text{h}\cdot\text{kg}^{-1}$  and volumetric energy density to  $1621.84 \text{ W}\cdot\text{h}\cdot\text{L}^{-1}$  [Fig. 4(b)]. Despite a small capacity reduction in the second cycle, the battery capacity shows a high retention of 78.2% in the third cycle. The energy density is  $711.3 \text{ W}\cdot\text{h}\cdot\text{kg}^{-1}$  and  $1653.65 \text{ W}\cdot\text{h}\cdot\text{L}^{-1}$  according to the third party testing report of parallel batteries as shown in Fig. S3. The volume change of the initial cell is only 5.09% after the first cycle.

In summary, through the application of advanced electrode materials and extreme manufacturing technology, we have manufactured  $10 \text{ A}\cdot\text{h}$ -level pouch-type rechargeable lithium batteries with ultra high energy density. The historical trajectory of yearly energy density record for practical rechargeable intercalation-type cathode cells is depicted in Fig. 4(c). The dashed line represents the present most advanced commercial lithium-ion batteries of  $360 \text{ W}\cdot\text{h}\cdot\text{kg}^{-1}$  first fabricated by Beijing WeLion New En-

ergy Technology Co., Ltd. The best record in laboratory is  $575 \text{ W}\cdot\text{h}\cdot\text{kg}^{-1}$  and  $1414 \text{ W}\cdot\text{h}\cdot\text{L}^{-1}$  created by the research group of Jeff Dahn.<sup>[8]</sup> We believe our work reaches both the highest gravimetric and volumetric energy density reported to date since the invention of lithium-ion batteries in the 1990s. However, we should note that there is always a contradictory among the energy density, cycling performance, rate performance, and safety in lithium batteries. Therefore, those parameters still need to be considered comprehensively to meet the demand of specific fields in the future. It is worth noting that the highest gravimetric energy density reported is  $685 \text{ W}\cdot\text{h}\cdot\text{kg}^{-1}$  for Li|O<sub>2</sub> battery (model battery)<sup>[29]</sup> and  $695 \text{ W}\cdot\text{h}\cdot\text{kg}^{-1}$  for Li|S battery (pouch type).<sup>[30]</sup> Nonetheless, the volumetric energy density for Li|Air and Li|S batteries available for query is no more than  $600 \text{ W}\cdot\text{h}\cdot\text{L}^{-1}$ , which is far less than that in advanced lithium ion batteries mentioned above. The batteries fabricated based on intercalation materials in this work exhibit priority when both high gravimetric and volumetric energy densities are required.

*Acknowledgments.* This work was supported by the National Key Research and Development Program of China (Grant No. 2021YFB2500300), the National Natural Science Foundation of China (Grant No. 22239003), the CAS Project for Young Scientists in Basic Research (Grant No. YSBR-058), and the Strategic Research and Consulting Project of the Chinese Academy of Engineering (Grant No. 2022-XZ-15). We sincerely thank Dr. Bitong Wang and Mr. Luyu Gan for their support in preparing the manuscript, and Mr. Mingwei Zan, Ms. Qiuchen Wang and Mr. Sichen Jiao for their support in experiments and data processing.

## References

- [1] Hiroshi K, Marcelo L, Kenneth I, and Hoi W J C 2021 United Nations, Department of Economic and Social Affairs: Economic Analysis *Frontier Technology Issues: Lithium-Ion Batteries: A Pillar for a Fossil Fuel-Free Economy*
- [2] Li Q, Yu X Q, and Li H 2022 *eTransportation* **14** 100201
- [3] 2021 U.S. Department of Energy National Blueprint for Lithium Batteries 2021–2030
- [4] Edström K 2022 *Battery 2030+ Inventing the Sustainable Batteries of the Future: Research Needs and Future Actions*, in *Roadmap paper*
- [5] Viswanathan V, Epstein A H, Chiang Y M, Takeuchi E, Bradley M, Langford J, and Winter M 2022 *Nature* **601** 519
- [6] 2021 U.S. Department of Energy's (DOE) Argonne National Laboratory White Paper: Assessment of the R&D Needs for Electric Aviation
- [7] Li W J, Xu H Y, Yang Q, Li J M, Zhang Z Y, Wang S B, Peng J Y, Zhang B, Chen X L, and Zhang Z 2020 *Energy Storage Sci. Technol.* **9** 448
- [8] Louli A J, Eldesoky A, deGooyer J, Coon M, Aiken C P, Simunovic Z, Metzger M, and Dahn J R 2022 *J. Electrochem. Soc.* **169** 40517
- [9] Usubelli C, Besli M M, Kuppan S, Jiang N N, Metzger M, Dinia A, Christensen J, and Gorlin Y 2020 *J. Electrochem. Soc.* **167** 080514
- [10] Lin D C, Liu Y Y, and Cui Y 2017 *Nat. Nanotechnol.* **12** 194
- [11] Yu L L, Tian Y X, Xiao X, Hou C, Xing Y R, Si Y H, Lu H, and Zhao Y J 2021 *J. Electrochem. Soc.* **168** 050516

- [12] Xu K 2004 *Chem. Rev.* **104** 4303
- [13] Cheng X B, Zhang R, Zhao C Z, and Zhang Q 2017 *Chem. Rev.* **117** 10403
- [14] Xu K 2014 *Chem. Rev.* **114** 11503
- [15] Kuang Y D, Chen C J, Kirsch D, and Hu L B 2019 *Adv. Energy Mater.* **9** 1901457
- [16] Niu C J, Lee H K, Chen S R, Li Q Y, Du J, Xu W, Zhang J G, Whittingham M S, Xiao J, and Liu J 2019 *Nat. Energy* **4** 551
- [17] Eldesoky A, Louli A J, Benson A, and Dahn J R 2021 *J. Electrochem. Soc.* **168** 120508
- [18] Pham M T M, Darst J J, Walker W Q, Heenan T M M, Patel D, Iacoviello F, Rack A, Olbinado M P, Hinds G, Brett D J L, Darcy E, Finegan D P, and Shearing P R 2021 *Cell Rep. Phys. Sci.* **2** 100360
- [19] Xiong R Y, Zhang Y, Wang Y M, Song L, Li M Y, Yang H, Huang Z G, Li D Q, and Zhou H M 2021 *Small Methods* **5** 2100280
- [20] Chang Z, Yang H J, Zhu X Y, He P, and Zhou H S 2022 *Nat. Commun.* **13** 1510
- [21] Chen J, Fan X L, Li Q, Yang H B, Khoshi M R, Xu Y B, Hwang S, Chen L, Ji X, Yang C Y, He H X, Wang C M, Garfunkel E, Su D, Borodin O, and Wang C S 2020 *Nat. Energy* **5** 386
- [22] Yin W, Grimaud A, Rousse G, Abakumov A M, Senyshyn A, Zhang L T, Trabesinger S, Iadecola A, Foix D, Giaume D, and Tarascon J M 2020 *Nat. Commun.* **11** 1252
- [23] Huang W Y, Yang L Y, Chen Z F, Liu T C, Ren G X, Shan P Z, Zhang B W, Chen S M, Li S N, Li J Y, Lin C, Zhao W G, Qiu J M, Fang J J, Zhang M J, Dong C, Li F, Yang Y, Sun C J, Ren Y, Huang Q Z, Hou G J, Dou S X, Lu J, Amine K, and Pan F 2022 *Adv. Mater.* **34** 2202745
- [24] Niu C J, Pan H L, Xu W, Xiao J, Zhang J G, Luo L L, Wang C M, Mei D H, Meng J S, Wang X P, Liu Z A, Mai L, and Liu J 2019 *Nat. Nanotechnol.* **14** 594
- [25] Louli A J, Eldesoky A, Weber R, Genovese M, Coon M, deGooyer J, Deng Z, White R T, Lee J, Rodgers T, Petibon R, Hy S, Cheng S J H, and Dahn J R 2020 *Nat. Energy* **5** 693
- [26] Ou X, Liu T C, Zhong W T, Fan X M, Guo X Y, Huang X J, Cao L, Hu J H, Zhang B, Chu Y S, Hu G R, Lin Z, Dahbi M, Alami J, Amine K, Yang C H, and Lu J 2022 *Nat. Commun.* **13** 2319
- [27] Cao W Z, Li Q, Yu X Q, and Li H 2022 *eScience* **2** 47
- [28] Cao X, Ren X D, Zou L F, Engelhard M H, Huang W, Wang H, Matthews B E, Lee H K, Niu C J, Arey B W, Cui Y, Wang C M, Xiao J, Liu J, Xu W, and Zhang J G 2019 *Nat. Energy* **4** 796
- [29] Kondori A, Esmailirad M, Harzandi A M, Amine R, Saray M T, Yu L, Liu T C, Wen J G, Shan N N, Wang H H, Ngo A T, Redfern P C, Johnson C S, Amine K, Shahbazian-Yassar R, Curtiss L A, and Asadi M 2023 *Science* **379** 499
- [30] Cheng Q, Chen Z X, Li X Y, Hou L P, Bi C X, Zhang X Q, Huang J Q, and Li B Q 2023 *J. Energy Chemistry* **76** 181